Food Hydrocolloids 163 (2025) 111024

Contents lists available at ScienceDirect

Food Hydrocolloids

journal homepage: www.elsevier.com/locate/foodhyd

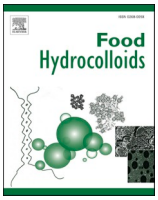

Controlled digestion of lipids from oil-laden core-shell beads with tunable core and shell design

Boxin Deng [a,*], Tom Kamperman [b], Vincent Rangel [b], Barbara Zoetebier-Liszka [b], Karin Schroën [a,1], Meinou Corstens [a,1]

[a] Wageningen University, Department of Agrotechnology & Food Sciences, Laboratory of Food Process Engineering Group, Bornse Weilanden 9, 6708 WG, Wageningen, the Netherlands

[b] IamFluidics B.V., De Veldmaat 17, 7522 NM, Enschede, the Netherlands

ARTICLE INFO

Keywords:
Lipid digestion
Lipolysis kinetics
Core-shell
Encapsulation
INFOGEST
In-air microfluidics

ABSTRACT

Lipid digestion products released and absorbed further down in the small intestine can induce feelings of satiety and reduce food intake. To achieve controlled lipolysis, uniformly sized core-shell beads were designed with different dimensions (i.e., oil core size and calcium-alginate hydrogel shell thickness) and compositions (i.e., wax addition in the oil core, chitosan and glutaraldehyde addition in the shell) through an in-air microfluidic technique. We investigated lipolysis from these beads under simulated oral, gastric, and intestinal conditions following the standardized INFOGEST *in vitro* digestion model. Lipolysis kinetics were monitored by image analysis of the core size and automatic titration of the lipolytic products – free fatty acids.

The hydrogel shell swells and remains intact throughout gastrointestinal incubation, while the lipid core shrinks due to lipid digestion. The lipolysis rate ($\mu mol \cdot s^{-1}$) scales linearly with the total lipid surface area, leading to a constant rate per unit of surface area of 14 μmol fatty acids$\cdot m^{-2} \cdot s^{-1}$. This unifies the results obtained for varied core sizes and oil doses. A delay in the onset of intestinal lipolysis was observed for core-shell beads of which the shell layer swells greatly under gastric and early-stage intestinal incubations. This swelling extends the pathway for intestinal lipase diffusion to the core surface, thus delaying the onset of lipid digestion, which can be as long as 60 min. Furthermore, we found that both core gelation (i.e., wax addition) and tightening the shell (i.e., additional cross-linking) greatly suppress the onset and rate of digestion. These insights can be used to predict and fine-tune the lipolysis behavior of core-shell beads, which paves the way for their rational application in functional (food) products, for example, to control food intake.

1. Introduction

Nutrients such as lipids that are released and absorbed in the (distal) small intestine can induce a hormonal feedback mechanism to trigger feelings of satiety and consequently a reduced food intake through the so called 'intestinal brake' mechanism (Golding & Wooster, 2010; Wilbrink, Masclee, Klaassen, et al., 2021). The intensity of the satiety signal has been shown to depend on the energy density of the components released. We consider this an important starting point for creating functional foods that may be used to target reduced food intake, which is ultimately important in the worldwide attempts to prevent obesity/overweight.

Lipid digestion (i.e., lipolysis) is a complex interfacial process. During lipid digestion, a series of interfacial interactions take place, including but not limited to, the binding of lipase onto the surface of emulsion droplets (Sarkar, Zhang, Holmes, et al., 2019) and the removal of lipolytic products from the surface of emulsion droplets (Acevedo-Fani & Singh, 2022; Scheuble, Schaffner, Schumacher, et al., 2018). The droplet size is the most important parameter that determines the rate of hydrolysis under digestive conditions (Corstens et al., 2017a). If emulsion droplets aggregate/flocculate or coalesce under digestive conditions, an appreciable variation in the droplet size (i.e., the accessible surface area) will be the consequence, leading to differences in lipolysis (Corstens et al., 2017b;McClements & Li, 2010; Scheuble, Schaffner, Schumacher, et al., 2018; Verkempinck et al., 2018a, 2018b). Therefore, to regulate lipid digestion (and eventually to control/reduce

* Corresponding author.
E-mail address: boxin.deng@wur.nl (B. Deng).
[1] Shared last authorship.

https://doi.org/10.1016/j.foodhyd.2024.111024
Received 11 October 2024; Received in revised form 9 December 2024; Accepted 24 December 2024
Available online 31 December 2024

food intake through rational design of emulsion droplets), it is crucial to ensure that emulsion droplets are physically stable within the gastrointestinal (GI) tract (McClements & Xiao, 2012; Tan et al., 2020b). Many researchers have focused on structuring the surface of emulsion droplets by using different types of surface-active components, ranging from surfactants to (nano-)particles (Lee, Jo, Jeong, et al., 2023; Ni, Gu, Li, et al., 2021), but in practically all cases this does not prevent bulk behaviors such as flocculation and coalescence from happening (Corstens et al., 2017c). An alternative approach is to encapsulate the emulsion droplets within a hydrogel matrix (e.g., alginate beads) (Lee & Mooney, 2012). In earlier work, we showed that depending on the polymer and the conditions used during the fabrication of alginate beads, various effects take place, ranging from structures that are resistant to the conditions in the GI tract, to their complete disintegration (Wu, Schroën, & Corstens, 2024).

Emulsion-filled alginate beads have been investigated for the controlled-release of fatty acids and bioactive components during lipid digestion (Chen, Deng, Zhang, et al., 2018; Corstens et al., 2017a; Corstens, Berton-Carabin, Schroën, et al., 2018; Zhang, Zhang, Zou, et al., 2016), and shown to reduce food intake in a proof-of-concept study (Corstens, Troost, Alleleyn, et al., 2019). In these studies, the rate and extent of lipid digestion are (considerably) lower for entrapped droplets as compared to free droplets (Han, Zhang, Shang, et al., 2020). Moreover, the properties of the beads, including the bead size and the degree of polymer cross-linking (also referred to as mesh size), largely determine the initiation, as well as the rate and extent of lipid digestion (Corstens et al., 2017a; Li, Hu, Du, et al., 2011; Rungraung, Jain, Mitbumrung, et al., 2022). Furthermore, these emulsion-filled alginate beads typically possess very limited transparency and contain high numbers of small droplets of which it is impossible to follow the individual digestion. These issues can be circumvented by using core-shell beads (one lipid droplet wrapped by one shell) that are promising candidates for characterizing the physiological processes taking place when monitoring the droplet size during lipid digestion (Hong & Salentinig, 2022; Patton & Carey, 1979). Although the core-shell beads have been reported to hold promise for biomedical and food-relevant applications (Galogahi, Zhu, An, et al., 2020; Wu, Zhang, Xu, et al., 2017), their potential in regulating lipid digestion has not been studied yet.

In the current study, our objective was to investigate if core-shell beads can be used to tune lipid digestion. Highly defined core-shell beads that are extremely uniform in their core and total size were produced by the in-air microfluidic technique that is suited to produce liters of product per hour (Visser, Kamperman, Karbaat, et al., 2018) and thus stands out from other microfluidic techniques (Schroën et al., 2022). Lipid digestion was monitored by chemical quantification of the lipolytic products (i.e., free fatty acids) and physical quantification via image analysis of the reducing size of the lipid droplets. We evaluated the impact of the core-shell designs – dimensions (e.g., core size and oil dose, as well shell thickness) and compositions, on the rate and extent of lipid digestion, following the standardized INFOGEST *in vitro* digestion model (Brodkorb et al., 2019). The obtained insights allowed us to conclude that core-shell beads hold great promise for controlled lipolysis and release through their flexibility in designs.

2. Experimental

2.1. Materials

Safflower oil (19200 High Linoleic Refined) which has been shown to induce the strongest feedback mechanisms (Maljaars, Romeyn, Haddeman, Peters, & Masclee, 2009) was obtained from De Wit Specialty Oils, the Netherlands. Carnauba wax (T1 flakes) was obtained from Koster Keunen Holland BV. Sodium alginate (80–120 cp, M/G ratio = 2.26 ± 0.17, Mw = 88.8 kDa) was obtained from FUJIFIM Wako Chemicals, Japan. Chitosan (Kitozyme chitosan of fungal origin; degree of acetylation: 0–30 %mol/wet weight; viscosity in 1% HAc: 1–15 mPa s, *i.e.* MW < 50 kDa) was obtained from Glentham Life Sciences. Glutaraldehyde, all enzymes including pepsin from porcine gastric mucosa (P7125), pancreatin from porcine pancreas (P7545, 8x USP specification, including trypsin, amylase, lipase, ribonuclease, protease), and lipase from pancreatin (L3126), the bovine bile extract (B3883, dried, unfractionated), as well as the chemicals that were used to prepare simulated saliva fluid (SSF), simulated gastric fluid (SGF), and simulated intestinal fluid (SIF), including sodium chloride (≥99.5%), calcium chloride dihydrate (≥99%), potassium phosphate monobasic (≥99%), magnesium chloride (≥98%), and ammonium carbonate (≥30% NH_3 basis), were obtained from Sigma Aldrich (St. Louis, USA). Potassium chloride was obtained from EMSURE (Merck KGaA, Germany). The sodium hydroxide (NaOH, ≥95%) and hydrochloric acid (HCl, 37–38%) were from Sigma Aldrich (St. Louis, MO, USA) and Actu-All Chemicals (Oss, NL), respectively. All solutions were prepared with ultrapure water (Millipore Corporation, Billerica, Massachusetts, USA).

2.2. Fabrication of core-shell beads

To produce core-shell beads, in-air microfluidics (IAMF) technique (Visser, Kamperman, Karbaat, et al., 2018), was chosen, because of its precision, and scalability compared to conventional chip-based microfluidics (Schroën et al., 2022). Successful production of monodisperse core-shell beads using IAMF has been previously demonstrated (Jiang, Poortinga, Liao, et al., 2023; Loo, Den, NunoAraújo-Gomes et al., 2023). The process is schematically illustrated in Fig. 1a. In brief, two nozzles were used: a vibrating coaxial nozzle to create a core/shell compound jet (nozzle 1 in Fig. 1a) and a nozzle to create a crosslinker jet (nozzle 2 in Fig. 1a). By vibrating the coaxial nozzle using an external actuator device that was driven by a waveform generator generating a sinus wave with a defined frequency between 100 and 1000 Hz, the liquid core/-shell compound jet was broken into a continuous stream of droplets (Fig. 1b). These droplets were covered with a crosslinking solution (10% ethanol and 200 mM $CaCl_2$) (Fig. 1c). Ethanol lowers the surface tension and thus drives the encapsulation process of the compound jet by the crosslinker jet, and crosslinking is initiated by the diffusion of Ca^{2+} ions from the crosslinker jet into the alginate layer (i.e., the shell), as previously described in detail by Visser, Kamperman, Karbaat, et al. (2018) (Fig. 1c). The rapid crosslinking kinetics of alginate with divalent cations are compatible with the production frequency (~1000/s), which ensures sufficient shell solidification before reaching the crosslinker bath and thus the circularity and dispersity of the core-shell beads. After production, the core-shell beads were stored in 200 mM $CaCl_2$ solution to ensure complete gelation. Since the beads were made using the same setup as described in the paper of Visser et al. (2018), we refer to that work for further technical details.

For formulations 1–3, pure safflower oil and 1.5% wt. sodium alginate in dH_2O were used to produce the regular beads with different core and shell sizes. To produce beads with shell modifications (formulations 4–6), a 1:1 mixture of 1.5% wt. sodium alginate (dH_2O) and 1.5% wt. chitosan (2% acetic acid solution in dH2O, pH 3–4) was used. Under this pH range, alginate has a negative charge and chitosan a (slightly) positive charge, so complex formation is expected. The beads are collected in a pH neutral calcium bath, with a shell composition of 0.75% wt. sodium alginate supplemented with 0.75% wt. chitosan and pure safflower oil as the core.

For formulation 5, the beads received a heat treatment to check their compatibility with typical pasteurization cycles used in food industry, using the method described by Smit, Keenan, Kovacs, et al. (2011). In brief, washed beads were mixed at 1:1 ratio with a 40 mM $CaCl_2$ solution. Heat resistant tubes were pre-heated to 72 °C (rate 10 °C/min) using water bath, and then beads were 30 s stirred at 65 °C for homogenization. Afterwards, the beads were pasteurized at 92 °C for 5 min, cooled to 42 °C for 5 h, pH adjusted to 4.6, and lastly, 30 s stirred for final homogenization.

For formulation 6, beads were post-crosslinked by overnight

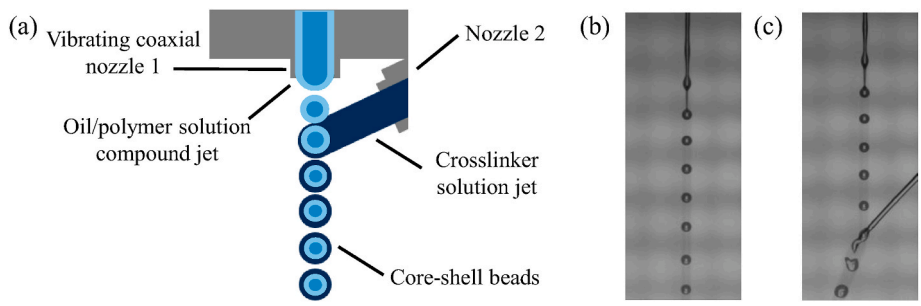

Fig. 1. Schematic illustration of the in-air microfluidic jetting system (a) and microscopic images from real experiments, showing the compound jet (b) and the coalescence of the compound jet with the crosslinker jet (c).

treatment with a 2.5% (w/v) glutaraldehyde solution and then heat treated. The use of glutaraldehyde is an academic exercise to check its effect and guide bead design, not to be used directly in practice given toxicity issues of the component.

To produce beads with core modification (formulation 7), safflower oil supplemented with 5% wt. carnauba wax was used, in conjunction with 1.5% wt. sodium alginate. Specifically, the wax/oil mixture was pre-heated and the compound jet was kept at a temperature of 50–60 °C. The crosslinker jet and bath were kept at a temperature of approximately 4 °C, to induce rapid bi-gel formation. Before adding to the digestion system, all beads were washed using ultrapure water to remove the excess calcium ions and free oil (if any).

Detailed information on the dimensions of the core-shell beads is shown in Table 1 d_{cs} represents the total diameter of the core-shell beads, d_c the core diameter, h_s the shell thickness, and φ the oil content of the core-shell beads. CV_{cs} and CV_c represent the coefficient of variation (CV) of the core-shell beads and the cores, respectively. These dimensional characteristics were obtained through image analysis of 5–15 beads (see section 2.4).

2.3. Determination of oil content

The oil content (φ, %) was estimated based on the dimensional characteristics of the core-shell beads (Table 1), namely by $\varphi\ (\%) = \frac{m_c}{m_{cs}} \times 100$, in which m_c and m_{cs} are the mass of the core and the whole core-shell bead, respectively. The densities of the core and the shell layer were assumed to be 0.921 and 1.012 g/mL, respectively, at room temperature. The obtained values were found to be slightly higher than those measured with the method described by Corstens et al. (2017a) for emulsion-filled beads, with a deviation of less than 15%.

2.4. Microscopic observation and image analysis

A light microscope (Axioscope, Zeiss, Germany) was used to monitor the integrity and the dimensional properties of the core-shell beads at selected time points throughout the gastrointestinal incubation. Images were recorded using 2.5× and 10× magnifications, with pixel size of 2.1868 and 0.5455 μm/pixel, respectively. To monitor changes in the bead and core diameter, as well as the shell thickness, images were analyzed using Image J software (version 1.51f). Image analysis was performed and averaged for 5–15 individual core-shell beads. At each time point during digestion, beads were temporarily sampled from the digestion system for quick microscopic observations.

2.5. In vitro gastrointestinal digestion

The *in vitro* gastrointestinal digestibility of core-shell beads was examined by incubating them with simulated digestive fluids: SSF (i.e., oral digestion), SGF (i.e., gastric digestion), and SIF (i.e., intestinal digestion), following the conditions of the standardized INFOGEST model (Brodkorb et al., 2019). In brief, a double-walled glass beaker was used as the reactor, and the digestion system was magnetically stirred at 240 rpm while its temperature being kept using a water bath set at 37 °C. The beads (containing 0.3 g lipid; total mass of beads in water was 5 g) were incubated in SSF (pH 7.0, 10 mL, 30 s), in SGF (pH 3.0, 20 mL, 2 h), and in SIF (pH 7.0, 40 mL, up to 5 h), following the electrolyte conditions described in the INFOGEST protocol. Upon transition between digestive phases, 0.2 M HCl and 0.5 M NaOH were used for pH adjustment, and in the intestinal phase, 0.1 M NaOH was used as the titrant (Metrohm Titrino 877, Metrohm Nederland, the Netherlands). In the intestinal phase, enzymes – pancreatin and additional lipase – were added (2000 U/mL lipolytic activity), and lipid digestion was monitored using both the image analysis (of the core size) and the titrated volume of NaOH (V_{NaOH}) using the so-called pH stat method that keeps the pH constantly at the same value. With the latter method, assuming that only fatty acids located at positions 1 and 3 on the backbone of glycerol can be released, the titrated volume of NaOH can be converted into the percentage of free fatty acids (FFA) released, using Eq. (1).

$$FFA\ (\%) = \left(\frac{V_{NaOH} \times m_{NaOH} \times M_{lipid}}{\omega_{lipid} \times 2}\right) \times 100\% \qquad \text{Eq. (1)}$$

In which, V_{NaOH}, in theory is the volume of NaOH that is titrated to neutralize the free fatty acids (in mL), m_{NaOH} its molar concentration (in M), M_{lipid} the averaged molecular weight of the lipid material (i.e., 874 g/mol for safflower oil), and ω_{lipid} the weight of the lipid initially added to the digestion system (in g). In practice, the titrated volume represents the total volume of NaOH consumed by the digestion system, which may include effects related to the titration of alginate shell and digestive

Table 1
The dimensional characteristics of the core-shell beads.

Formulation	Sample name	Total diameter d_{cs} (μm)	Core diameter d_c (μm)	Shell thickness h_s (μm)	Oil content φ (% v/v)	CV_{cs} (%)	CV_c (%)
1	ALG-620cores	920	620	150	28	1.2	1.7
2	ALG-510cores	810	510	150	23	2.4	1.0
3	ALG-295cores	485	295	95	22	2.5	1.0
4	ALG-CS	920	550	185	20	3.0	1.2
5	ALG-CS-heated	820	550	135	28	2.7	1.2
6	ALG-CS-GA	930	550	190	20	2.3	1.3
7	ALG-wax	860	530	165	22	1.2	1.9

fluids. Therefore, we performed blank measurements to estimate the NaOH consumption by empty alginate beads and digestive fluids. Corrections of the V_{NaOH} values (and thereafter the FFA percentages) were carried out using these blank values (see Fig. 4 for illustration).

We evaluated the impact of bead design and composition on lipolysis of core-shell beads. For the investigation of the core diameter and the shell thickness, we used calcium-alginate hydrogel – oil core beads with different geometry (formulations 1–3), with the oil dose fixed at 0.3 g lipid. For the investigation of the oil dose (0.15, 0.3 and 0.6 g lipid), we used sample ALG-295cores. For the investigation of the modified composition of shell and core, we used formulations 4–7, with a fixed oil dose of 0.3 g lipid. Each digestion experiment was repeated two to five times. During all experiments, we took care that the core-shell beads were evenly distributed in the digestive fluids; throughout gastrointestinal incubation creaming and flocculation were not observed.

3. Results & discussion

In this section, we first introduce the microfluidic approach used for the production of core-shell beads (section 3.1). In section 3.2, we describe the lipolysis of core-shell beads under gastrointestinal conditions as function of digestive time for up to 7 h. In section 3.3 and 3.4, we study the impact of the core size, and the amount of lipid used, respectively, which we connect to the total lipid surface area available in section 3.5.1. The functional role of the shell layer (i.e., hydrogel matrix) in lipid digestion is discussed in section 3.5.2. Lastly, in section 3.5.3, we study the potential of modulating lipolysis through varying core and shell compositions.

3.1. Engineering production of core-shell beads

To produce core-shell beads, in-air microfluidics (IAMF) was chosen, because of its precision, and scalability compared to conventional chip-based microfluidics (Schroën et al., 2022). In line with previous studies using in-air microfluidics, the size of the core, the shell, and also the whole bead could be readily tuned by changing the nozzle size, total flow rate, and flow rate ratio (Kamperman, Loo, Gurian, et al., 2019), as well as the nozzle vibration frequency (Visser, Kamperman, Karbaat, et al., 2018). As shown in Table 1, this droplet-microfluidic approach allows for production of monodisperse core-shell beads with highly defined dimensions (with CV $<$ 5%) and compositions.

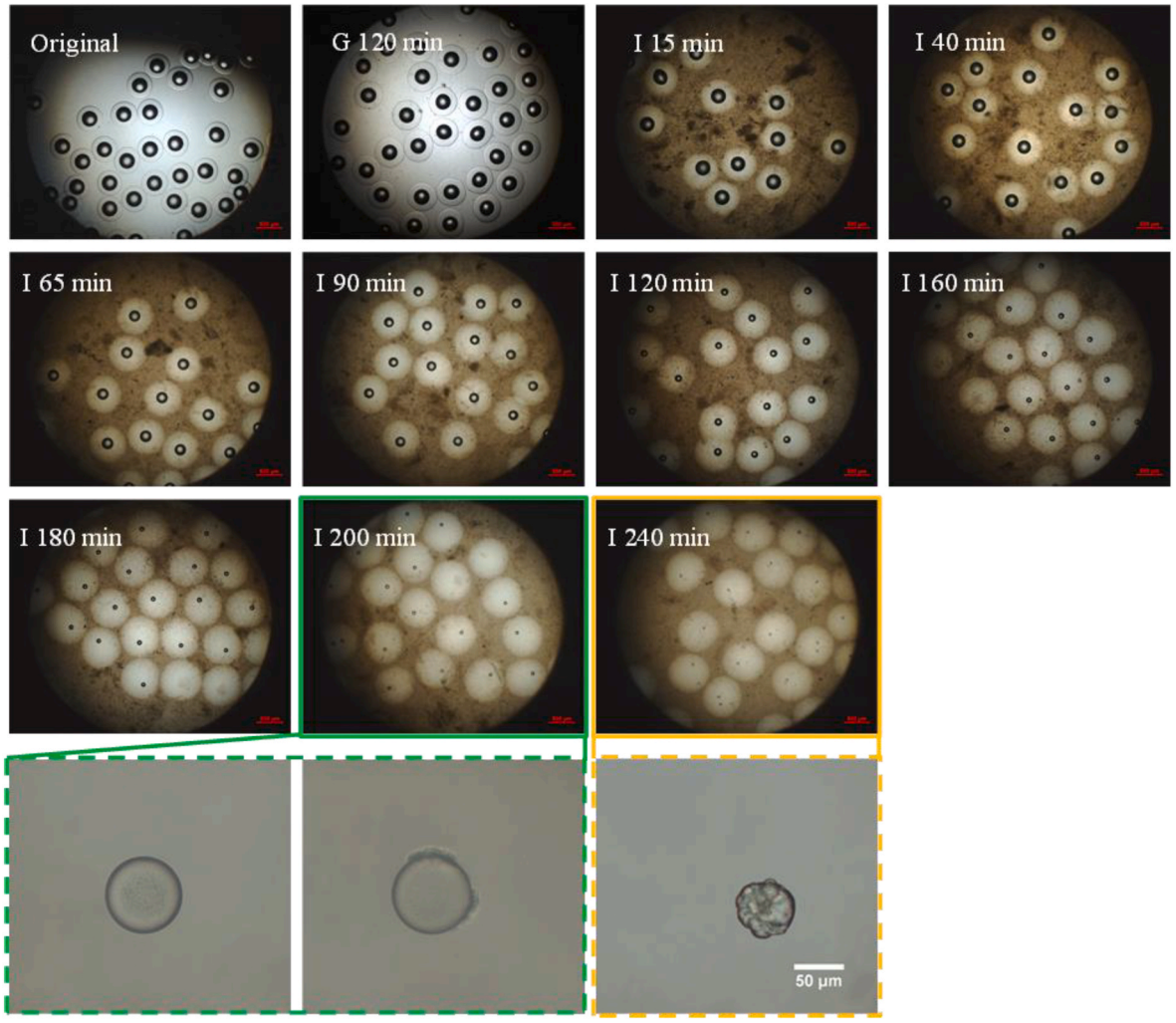

Fig. 2. Microscopic observations of core-shell beads incubated under gastric and intestinal conditions. Recordings were made at selected time points (G: gastric, I: intestinal). These images were recorded for core-shell beads ALG-295cores, and the oil dose for this experiment was 0.3 g lipid. First three rows of images, the scale bar is 500 µm. Last row of images (zoomed-in observations for I 200 min (green) and I 240 min (yellow), respectively): wrinkled surfaces observed when lipolysis approaches an end. It was noted that only a few cores start developing a wrinkled surface at t = 200 min, while at t = 240 min, all the cores have a wrinkled surface. (For interpretation of the references to colour in this figure legend, the reader is referred to the Web version of this article.)

3.2. The digestion of lipid encapsulated within core-shell beads

We then studied the lipolysis of core-shell beads under gastrointestinal conditions as a function of incubation time. Fig. 2 shows the microscopic observations at selected time points throughout gastrointestinal incubation when using bead ALG-295cores. The core volume reduces during intestinal incubation, which is due to hydrolysis of the core triglycerides that are transferred into the digestive fluid in the form of monoglycerides and fatty acids.

We monitored the reduction in core diameter to quantify lipid digestion and compared this to the conventional titration method. As lipid digestion proceeds with time during intestinal incubation, the core diameter reduces linearly (Fig. 3a and Figure SI 1). The released fatty acids are neutralized by titration with NaOH (to keep the pH constant at 7.0), and the titrated volume of NaOH increases accordingly (Figure SI 2). Yet, in Fig. 4, the core volume reduction profile (pink, filled circles) and the free fatty acid (FFA) release profile (pink line) are systematically apart. The difference is expected to be mainly caused by NaOH needed to neutralize the alginate shell and the digestive fluids. This highlights the importance of carrying out proper blank measurements when titration method is used, as was also recently suggested by Okuro, Viau, Marze, et al. (2023). When this was taken into account (pink dashed line), the two datasets are in very good agreement, which proves the complementary nature of the two approaches in quantifying lipid digestion. In contrast to the titration method, the quantification of core volume is not affected by the blank measurements and has our preference to report on. The data on FFA release profiles are shown in Figure SI 3.

The shell layer swells and remains intact during gastric incubation at pH 3 and intestinal incubation at pH 7, as seen in Fig. 2. As a consequence, the shell thickness increases with time throughout the gastrointestinal incubation (Fig. 3b). While most literature relates the swelling behavior to the pH conditions (Li, Hu, Du, et al., 2011), it is also affected by the ionic environment (Ching, Bansal, & Bhandari, 2017; Malektaj, Drozdov, & Christiansen, 2023). The swelling behavior is most probably a response to the reduced calcium concentration in the digestive fluids (1.5, 0.15, or 0.6 mM in the oral, gastric, or intestinal phase, respectively) compared to the calcium concentration used during storage (200 mM $CaCl_2$). Besides, ion exchange between Ca^{2+} and Na^{+} has been reported to lead to swelling and even disintegration of the alginate gel (Bajpai & Sharma, 2004; Corstens et al., 2017a), depending on the M/G ratio of the alginate used (Lee, Ravindra, & Chan, 2013; Wu et al., 2024). In the current study, no disintegration was observed. However, a few cores escaped from the shells at the end of intestinal incubation, which is a point of improvement taken into account in future bead designs. Last but not least, we observed that the distance between the shell and the core increases during intestinal incubation (as indicated by the white arrow in the inset in Fig. 3b), which we further describe in section 3.5.2.

When the core volume is reduced to less than 2% of the original volume, we noticed that the initially spherical core gets dimpled and crumpled (see the last row in Fig. 2). In literature, this was also reported, for example, when a nanoparticle-laden bubble was subjected to (bubble) surface area reduction (Eftekhari, Schwarzenberger, Heitkam, et al., 2021). In this study, the wrinkled surface is formed most likely due to the irreversible adsorption of e.g., insoluble reaction products (i.e., Ca^{2+} soaps of free fatty acids or bile salts) (Mulet-Cabero & Wilde, 2023; Torcello-Gómez, Boudard, & Mackie, 2018; Zangenberg, Mullertz, Kristensen, et al., 2001), or insoluble matter from pancreatin and bile extract. The formation of wrinkled surface is seen as an indication of full digestion, since it occurs at a very small amount of residual lipid.

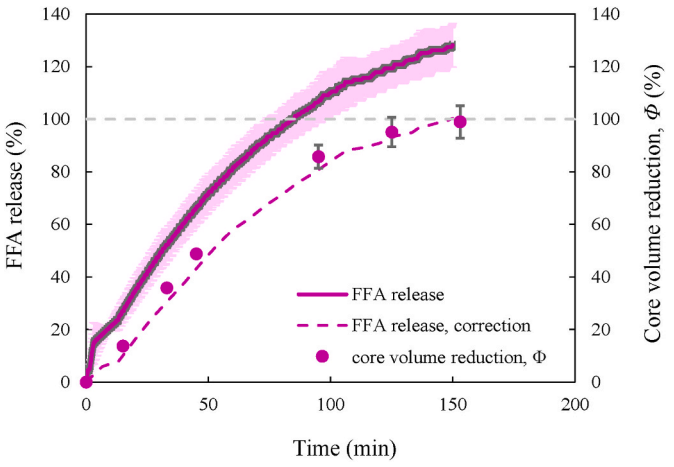

Fig. 4. A comparison of FFA release (pink lines) and core volume reduction (filled circles) versus intestinal incubation time. Error bars are invisible when they are smaller than the symbols. The FFA profile was further corrected for blank measurements (dashed pink line). These data were obtained for bead ALG-295cores and oil dose of 0.15 g lipid. (For interpretation of the references to colour in this figure legend, the reader is referred to the Web version of this article.)

3.3. The impact of core diameter

For smaller cores, a faster lipolysis (i.e., a steeper initial slope) and a larger extent of lipid digestion are observed throughout the intestinal incubation period (see Fig. 5a). For larger cores, the available lipid surface area is smaller when using an equal dose of lipid. The lipolysis kinetics are relatively slow for the large cores, as expected in the presence of a surplus of lipase and observed for free emulsion droplets (Tan et al., 2020a). Furthermore, for larger cores, a striking observation is the obvious 'delay' in the onset of lipid digestion (e.g., $\phi \sim 0\%$ at $t < 30$ min for 620 μm cores), which we relate to the functional role of the shell

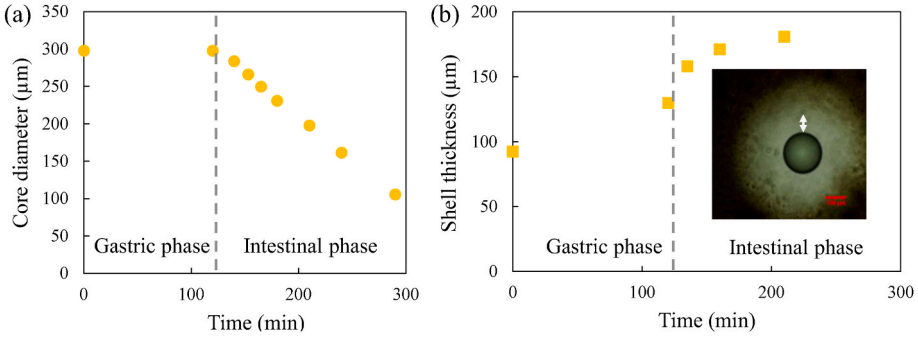

Fig. 3. The changes in the core diameter(a) and the shell thickness (b) versus digestion time in GI tract. In a, error bars are invisible since they are smaller than the symbols. In a, b, the gastric and intestinal phases are distinguished by a vertical dashed line, and in b, the inset image was recorded for I 90 min. In the inset image, the white arrow indicates the distance between the shell and the core. These data were obtained for bead ALG-295cores and oil dose of 0.3 g lipid. The scale bar is 100 μm.

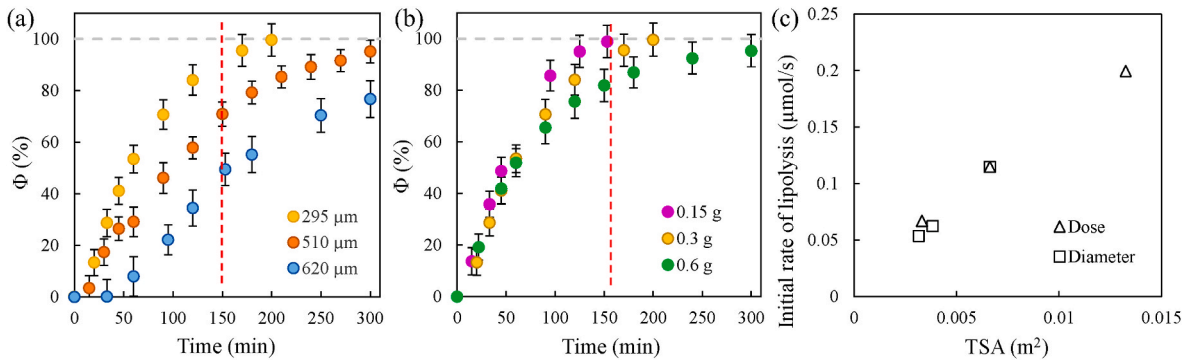

Fig. 5. The quantification of core volume reduction as function of the intestinal incubation time (up to 5 h) for different core diameters (a) and oil doses (b). In a and b, each data point represents an average value obtained for 15 beads. The vertical red dashed lines mark 2.5 h of intestinal incubation, which is mostly used as the last monitoring point following the standardized INFOGEST digestion model. The horizontal grey dashed lines mark full digestion. c. The initial rate of lipolysis as function of the total surface area (TSA) given for various oil dose and core diameter. These initial rates (μmol/s) are the initial slopes obtained from Figure SI 4. (For interpretation of the references to colour in this figure legend, the reader is referred to the Web version of this article.)

layer that we describe further in section 3.5.1.

3.4. The impact of lipid content (i.e., the dose)

At early stages of intestinal incubation, the initial rate of lipolysis and the extent of lipid digestion seem rather independent of the dose (Fig. 5b). At longer times, the lipolysis rate seems higher for the lower oil dose (transition at t = 60 min which is more clearly seen in Figure SI 1b) leading to a larger reduction in the core volume (e.g., at t = 150 min). However, when looking at the digested volume of the cores, it does increase linearly with the oil dose (Figure SI 5). These observations indicate an identical interfacial composition concerning the presence of e.g., *bile salts* that co-determine the interfacial adsorption of lipase (Macierzanka, Torcello-Gómez, Jungnickel, et al., 2019), but at higher dose a potential exhaustion of bile salts in the digestive fluids. This limits the solubilization and removal of surface active lipolytic products that might displace the adsorbed materials (e.g., lipase) from the core surface and eventually influence the continuation of lipid digestion (i.e., the rate and the extent of lipolysis) (Sarkar, Ye, & Singh, 2016).

3.5. The mechanism for controlled lipolysis

3.5.1. The role of total surface area available

The lipolysis process is a surface related reaction, and the core diameter as well as the oil dose used are both related to the total surface area (TSA) of lipid available. To capture the impact of TSA on lipid digestion, we converted the percentages of core volume reduction into the absolute amount of FFA released (in μmol) using two free fatty acids released from one triglyceride molecule (Figure SI 4). The initial rate of lipolysis – the initial slope of FFA (μmol) *vs.* time plot (excluding the lag phase), is found to scale linearly with the TSA obtained at t = 0 min (Fig. 5c). This implies no additional impact from core diameter and oil dose on top of TSA. The lipolysis rate per unit of surface area is obtained through a linear regression analysis of Fig. 5c. Results show that lipolysis in all systems takes place with a rate of approximately 14 μmol FFA·m^{-2}·s^{-1} (as soon as lipolysis sets of), which is an important parameter when comparing data on digestion of oil droplets in literature. The fact that all data comes together in a master curve indicates that the current hydrogel shell did not pose a diffusional limitation to lipase apart from the additional distance that the enzymes need to travel as discussed in the next section. If diffusion limitation occurs, the movement of enzyme molecules into the beads is influenced, and through that the rate and extent of lipid digestion (Li, Hu, Du, et al., 2011). In earlier work that revolved around gels with small sized emulsion droplets, this was discussed in terms of the relative magnitude of the mesh size of the gel and the size of enzyme molecules (Corstens et al., 2017a; van Leusden, den Hartog, Bast, et al., 2018; Wooster, Acquistapace, Mettraux, et al., 2019; Zhang, Qu, Zhou, et al., 2022).

3.5.2. The functional role of the hydrogel matrix

In contrast to the rate of lipolysis (after the onset), we hypothesize that lipase diffusion does play a role in the delayed onset of lipid digestion. The shell layer swells throughout the gastrointestinal incubation (Fig. 6), and the distance between the shell and the core (i.e., the liquid layer surrounding the core, as indicated by the white area in Fig. 6c) increases specifically during intestinal incubation due to shell swelling, both of which extend the pathway for lipase diffusion at early stages of intestinal incubation. The shell thickness increases more for larger cores, due to the larger (initial) shell volume. Beads with 620 μm cores have a 6-times larger shell volume than those with 295 μm cores before entering the GI tract (Figure SI 6a). The thickness of the liquid layer increases proportionally with time, showing no dependency on the core diameter at early stages of intestinal incubation (Figure SI 6b). Upon transfer from gastric phase to intestinal phase, lipase needs to diffuse through the shell and then the liquid layer to initiate lipid digestion that commences immediately upon the arrival of lipase at the core surface.

The effective distance that lipase needs to travel is influenced by the tortuosity of the hydrogel matrix that increases the path length (Lavrentev, Shilovskikh, Alabusheva, et al., 2023). As shown in Appendix 6, for a diffusion time of 15 min, the diffusional distance of lipase is comparable to the absolute shell thickness of the 920 μm beads achieved after gastric incubation and intestinal incubation for 15 min (when assuming the viscosity of the digestive fluid in these beads resembles that of water, see Figure SI 7. If the distance is longer (i.e., the prolonged path length due to the tortuosity of the hydrogel matrix), or the viscosity of the digestive fluid is higher than that of water, the arrival of lipase at the core surface during early stages of intestinal incubation will be further retarded. This explains the delay in the onset of lipid digestion (i.e., $\phi \sim 0\%$ at t < 30 min) as observed for the 920 μm beads with 620 μm cores.

3.5.3. The impact of core and shell composition

The digestion behavior of the core-shell beads can be further modulated by adjusting the shell or core composition. When chitosan was introduced to the shells (*abbr.* ALG-CS), a delay in lipolysis was observed, and subsequently, lipolysis takes place at appreciable rates comparable to some of the non-modified beads (triangles in Fig. 7). Once lipolysis starts after the onset, the lipolysis rate of these modified beads is determined by the core properties (i.e., the total surface area available, as previously discussed in section 3.5.1). Moreover, the shell layer is resistant to swelling throughout gastrointestinal incubation (see

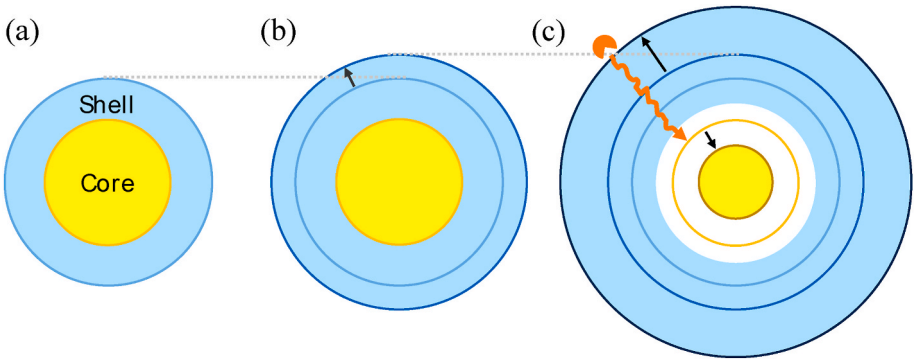

Fig. 6. Schematic illustration of the swelling behaviour of the shell layer and the reduction in core volume. Light, medium and dark blue circles represent the shell surface of the original bead (a), and that of the beads incubated for e.g., G 120 min (b) and I 90 min (c), respectively. Accordingly, light and dark yellow circles represent the core surface of the beads incubated for G 120 min and I 90 min, respectively. White area represents the liquid layer between the shell and the core. Arrows indicate the movement direction of the surface. The prolonged path length (orange line) for enzyme (orange symbol) diffusion is also sketched. The grey dashed lines are added to guide the eyes, and the sketch is not drawn to scale. (For interpretation of the references to colour in this figure legend, the reader is referred to the Web version of this article.)

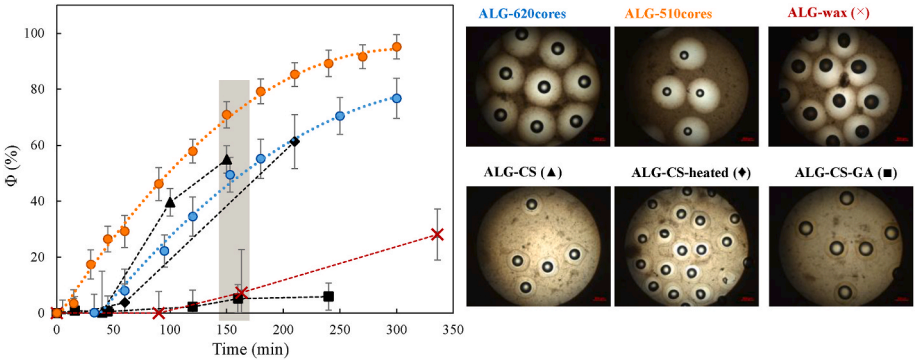

Fig. 7. The quantification of core volumes as function of intestinal incubation time (for up to 5 h) for core-shell beads with modified shells and cores, and some non-modified beads for comparison (data ALG-620cores and ALG-510cores are the same as in Fig. 5). The dotted lines are added to guide the eye. On the right, one representative image recorded after intestinal incubation at about 160 min (marked with grey rectangle in the graph on the left) or 210 min for 'ALG-CS-heated' is shown for different modifications. The scale bar for these images is 500 μm. Abbreviations represent: ALG – alginate, CS – chitosan, and GA – glutaraldehyde.

Fig. 7), unlike the non-modified beads discussed in section 3.2. This implies that the modified shell has increased diffusional resistance due to the enhanced crosslinking of alginate by both Ca^{2+} ions and chitosan (with its G- and M-blocks, respectively (Feng, Kopplin, Sato, et al., 2017)), which is an effect that surpasses that created by the swollen non-modified beads. Lastly, the aforementioned observations also hold when the beads were given a heat treatment (diamond symbols), implying that the beads can be pasteurized without losing their functionality. This is unique compared to many emulsion systems that lose functionality upon thermal treatment, including the previously commercialized Fabuless (Smit, Keenan, Kovacs, et al., 2011).

When beads were further treated with glutaraldehyde (*abbr.* ALG-CS-GA), digestion was very much delayed and suppressed (squares in Fig. 7). This is a clear indication that the shell has become much less permeable for the digestive components, most probably because of the reduced pore size that hinders diffusion of digestive components (Berger, Reist, Mayer, et al., 2004; Feyisa, Gupta, Edossa, et al., 2023). Some pores may even be small enough to retain these components and thus retard e.g., the transport of bile salts that are responsible for the removal of lipolytic products from the droplet surface (Sarkar et al., 2016).

When modifying the core with carnauba wax, lipolysis is delayed and suppressed almost as extremely as for shell modification with glutaraldehyde (Fig. 7, cross symbols). These observations align with literature, showing slower digestion of oleogels (Li, Lu, Yu, et al., 2023) or gelled emulsion droplets (Guo, Wijarnprecha, Sonwai, et al., 2019) compared to liquid oils. The wax crystallites/aggregates may either locate at the droplet (core) surface, creating a densely stacked interfacial film, or distribute in the core forming a *gel-like* less digestible network (Patel, Babaahmadi, Lesaffer, et al., 2015; Wang, Wang, Hou, et al., 2023), or a combination thereof. The delayed and suppressed lipolysis is likely due to shell swelling (as described in section 3.5.2), and most importantly, to a reduction of available lipid surface area for digestion (Ashkar, Laufer, Rosen-Kligvasser et al., 2019), by roughly 3-times, or a reduction of lipolysis rate because of effects on the digestive components, either directly (e.g., binding to the interface by enzymes) or indirectly (e.g., reduced removal of fatty acids by bile salts) (Dong, Lv, Gao, et al., 2020).

To summarize, the core-shell structure maintains the monodispersity of the lipid droplets and lipolysis rate scales with the total lipid surface area available. This uniquely prevents bulk effects that would occur with free emulsion droplets (i.e., flocculation/aggregation/coalescence) (Bellesi, Martinez, Ruiz-Henestrosa et al., 2016; Bourlieu-Lacanal, Ménard, Chevasnerie, et al., 2015). Such bulk effects would lead to reduced lipid digestion through physical instability (Verkempinck et al., 2018a, 2018b), which is an effect that is not often taken into consideration when discussing lipolysis rates of emulsions and encapsulates in literature. The specific design of the core-shell structure enables us to truly quantitatively investigate lipid digestion, as well as to unravel the exact role of the hydrogel matrix and the core/shell composition in controlling lipolysis. These are crucial leads for the design of core-shell beads (e.g., dimension and composition) and their addition to products (e.g., functional foods) for a well-controlled lipolysis profile for satiety

induction.

4. Conclusion

In this work, core-shell beads were engineered to control lipid digestion. In-air microfluidics was used to produce these beads. The impact of the dimensional and compositional design of core-shell beads on the rate (and extent) of lipid digestion was investigated under simulated gastrointestinal conditions, following the standardized INFOGEST *in vitro* digestion model.

The core-shell beads are featured with monodispersed cores and transparent shells. These features allow us to visualize and quantify lipid digestion on a single *drop-level*. Lipid digestion was quantified through the core volume reduction, and it was found that fatty acid release scales linearly with the total surface area available, which is a function of the size and the dose of the cores. Besides, the shell layer delays the onset of lipid digestion through shell swelling during gastric and early-stage intestinal incubations, which creates a longer pathway for lipase diffusion (to travel to the core surface and thus initiate lipolysis). Moreover, we proved that compositional modifications to the core and/or the shell can be used to further modulate lipolysis. Tightening the shell through cross-linking as well as core gelation largely delayed and suppressed lipolysis. We also proved the heat compatibility of our core-shell beads, which is very promising (e.g., in terms of post-processing such as pasteurization for food production) and brings the core-shell beads further toward applications in functional (food) products. The observations can be used to rationally design core-shell beads for controlled lipolysis and induction of the 'intestinal brake', as well as targeted delivery of bioactives dissolved in the encapsulated oil.

CRediT authorship contribution statement

Boxin Deng: Writing – original draft, Visualization, Methodology, Investigation, Formal analysis, Data curation, Conceptualization. **Tom Kamperman:** Writing – review & editing, Methodology, Funding acquisition, Conceptualization. **Vincent Rangel:** Methodology, Data curation. **Barbara Zoetebier-Liszka:** Writing – review & editing, Conceptualization. **Karin Schroën:** Writing – review & editing, Supervision, Methodology, Funding acquisition. **Meinou Corstens:** Writing – review & editing, Supervision, Methodology, Funding acquisition, Conceptualization.

Declaration of competing interest

The authors declare that they have no known competing financial interests or personal relationships that could have appeared to influence the work reported in this paper.

Acknowledgement

The authors would like to acknowledge European Fund for Regional Development (EFRO), OP-Oost PROJ-01112 for the financial support of this research.

Appendix A. Supplementary data

Supplementary data to this article can be found online at https://doi.org/10.1016/j.foodhyd.2024.111024.

Data availability

Data will be made available on request.

References

Acevedo-Fani, A., & Singh, H. (2022). Biophysical insights into modulating lipid digestion in food emulsions. *Progress in Lipid Research, 85*, Article 101129. https://doi.org/10.1016/j.plipres.2021.101129

Ashkar, A., Laufer, S., Rosen-Kligvasser, J., et al. (2019). Impact of different oil gelators and oleogelation mechanisms on digestive lipolysis of canola oil oleogels. *Food Hydrocolloids, 97*, Article 105218. https://doi.org/10.1016/j.foodhyd.2019.105218

Bajpai, S. K., & Sharma, S. (2004). Investigation of swelling/degradation behaviour of alginate beads crosslinked with ca2+ and ba2+ ions. *Reactive & Functional Polymers, 59*, 129–141.

Bellesi, F. A., Martinez, M. J., Ruiz-Henestrosa, V. M. P., et al. (2016). Comparative behavior of protein or polysaccharide stabilized emulsion under in vitro gastrointesinal conditions. *Food Hydrocolloids, 52*, 47–56. https://doi.org/10.1016/j.foodhyd.2015.06.007

Berger, J., Reist, M., Mayer, J. M., et al. (2004). Structure and interactions in covalently and ionically crosslinked chitosan hydrogels for biomedical applications. *European Journal of Pharmaceutics and Biopharmaceutics, 57*, 19–34. https://doi.org/10.1016/S0939-6411(03)00161-9

Bourlieu-Lacanal, C., Ménard, O., Chevasnerie, A. D. L., et al. (2015). The structure of infant formulas impacts their lipolysis, proteolysis and disintegration during in vitro gastric digestion. *Food Chemistry, 182*, 224–235. https://doi.org/10.1016/j.foodchem.2015.03.001

Brodkorb, A., Lotti Egger, M. A., Alvito, P., et al. (2019). Infogest static in vitro simulation of gastrointestinal food digestion. *Nature Protocols, 14*, 991–1014. https://doi.org/10.1038/s41596-018-0119-1

Chen, F., Deng, Z., Zhang, Z., et al. (2018). Controlling lipid digestion profiles using mixtures of different types of microgel: Alginate beads and carrageenan beads. *Journal of Food Engineering, 238*, 156–163. https://doi.org/10.1016/j.jfoodeng.2018.06.009

Ching, S. H., Bansal, N., & Bhandari, B. (2017). Alginate gel particles-a review of production techniques and physical properties. *Critical Reviews in Food Science and Nutrition, 57*(6), 1133–1152. https://www.ncbi.nlm.nih.gov/pubmed/25976619.

Corstens, M. N., Berton-Carabin, C. C., Elichiry-Ortiz, P. T., et al. (2017a). Emulsion-alginate beads designed to control in vitro intestinal lipolysis: Towards appetite control. *Journal of Functional Foods, 34*, 319–328. https://doi.org/10.1016/j.jff.2017.05.003

Corstens, M. N., Berton-Carabin, C. C., Kester, A., et al. (2017b). Destabilization of multilayered interfaces in digestive conditions limits their ability to prevent lipolysis in emulsions. *Food Structure, 12*, 54–63. https://doi.org/10.1016/j.foostr.2016.07.004

Corstens, M. N., Berton-Carabin, C. C., Schroën, K., et al. (2018). Emulsion encapsulation in calcium-alginate beads delays lipolysis during dynamic in vitro digestion. *Journal of Functional Foods, 46*, 394–402. https://doi.org/10.1016/j.jff.2018.05.011

Corstens, M. N., Berton-Carabin, C. C., Vries, R.d., et al. (2017c). Food-grade micro-encapsulation systems that may induce satiety via delayed lipolysis: A review. *Critical Reviews in Food Science and Nutrition, 57*(10), 2218–2244. https://www.ncbi.nlm.nih.gov/pubmed/26252442.

Corstens, M. N., Troost, F. J., Alleleyn, A. M. E., et al. (2019). Encapsulation of lipids as emulsion-alginate beads reduces food intake: A randomized placebo-controlled cross-over human trial in overweight adults. *Nutrition Research, 63*, 86–94. https://doi.org/10.1016/j.nutres.2018.12.004

Dong, L., Lv, M., Gao, X., et al. (2020). In vitro gastrointestinal digestibility of phytosterol oleogels: Influence of self-assembled microstructures on emulsification efficiency and lipase activity. *Food & Function, 11*, 9503. https://doi.org/10.1039/D0FO01642J

Eftekhari, M., Schwarzenberger, K., Heitkam, S., et al. (2021). Interfacial behavior of particle-laden bubbles under asymmetric shear flow. *Langmuir, 37*, 13244–13254. https://doi.org/10.1021/acs.langmuir.1c01814

Feng, Y., Kopplin, G., Sato, K., et al. (2017). Alginate gels with a combination of calcium and chitosan oligomer mixtures as crosslinkers. *Carbohydrate Polymers, 156*, 490–497. https://doi.org/10.1016/j.carbpol.2016.09.006

Feyisa, Z., Gupta, N. K., Edossa, G. D., et al. (2023). Fabrication of ph-sensitive double cross-linked sodium alginate/chitosan hydrogels for controlled release of amoxicillin. *Polymer Engineering & Science, 63*, 2546–2564. https://doi.org/10.1002/pen.26395

Galogahi, F. M., Zhu, Y., An, H., et al. (2020). Core-shell microparticles: Generation approaches and applications. *Journal of Science: Advanced Materials and Devices, 5*, 417–435. https://doi.org/10.1016/j.jsamd.2020.09.001

Golding, M., & Wooster, T. J. (2010). The influence of emulsion structure and stability on lipid digestion. *Current Opinion in Colloid & Interface Science, 15*, 90–91. https://doi.org/10.1016/j.cocis.2009.11.006

Guo, Q., Wijarnprecha, K., Sonwai, S., et al. (2019). Oleogelation of emulsified oil delays in vitro intestinal lipid digestion. *Food Research International, 119*, 805–812. https://doi.org/10.1016/j.foodres.2018.10.063

Han, J., Zhang, Z., Shang, W., et al. (2020). Modulation of physicochemical stability and bioaccessibility of β-carotene using alginate beads and emulsion stabilized by scallop (patinopecten yessoensis) gonad protein isolates. *Food Research International, 129*, Article 108875. https://doi.org/10.1016/j.foodres.2019.108875

Hong, L., & Salentinig, S. (2022). Functional food colloids: Studying structure and interactions during digestion. *Current Opinion in Food Science, 45*, Article 100817. https://doi.org/10.1016/j.cofs.2022.100817

Jiang, J., Poortinga, A. T., Liao, Y., et al. (2023). High-throughput fabrication of size-controlled pickering emulsions, colloidosomes, and air-coated particles via clog-free jetting of suspensions. *Advanced Materials, 35*, Article 2208894.

Kamperman, T., Loo, B.v., Gurian, M., et al. (2019). On-the-fly exchangeable microfluidic nozzles for facile production of various monodisperse micromaterials. *Lab on a Chip, 19*, 1977. https://doi.org/10.1039/C9LC00054B

Lavrentev, F. V., Shilovskikh, V. V., Alabusheva, V. S., et al. (2023). Diffusion-limited processes in hydrogels with chosen applications from drug delivery to electronic components. *Molecules, 28*. https://doi.org/10.3390/molecules28155931

Lee, S., Jo, K., Jeong, S.-K.-C., et al. (2023). Strategies for modulating the lipid digestion of emulsions in the gastrointestinal tract. *Critical Reviews in Food Science and Nutrition*. https://doi.org/10.1080/10408398.2023.2215873

Lee, K. Y., & Mooney, D. J. (2012). Alginate: Properties and biomedical applications. *Progress in Polymer Science, 37*, 106–126. https://doi.org/10.1016/j.progpolymsci.2011.06.003

Lee, B.-B., Ravindra, P., & Chan, E.-S. (2013). Size and shape of calcium alginate beads produced by extrusion dripping. *Chemical Engineering & Technology, 36*, 1627–1642. https://doi.org/10.1002/ceat.201300230

Li, Y., Hu, M., Du, Y., et al. (2011). Control of lipase digestibility of emulsified lipids by encapsulation within calcium alginate beads. *Food Hydrocolloids, 25*(1), 122–130. https://doi.org/10.1016/j.foodhyd.2010.06.003

Li, J., Lu, Y., Yu, N., et al. (2023). A depth-insight on reduced lipolysis of diacylglycerol (dag) oleogels with the gelation of diosgenin (dsg). *International Journal of Food Science and Technology, 58*, 2934–2941. https://doi.org/10.1111/ijfs.16402

Loo, B.v., Den, S. A.t., Nuno, A.-G., et al. (2023). Mass production oflumenogenic human embryoid bodies and functional cardiospheres using in-air-generated microcapsules. *Nature Communications, 14*, 6685. https://doi.org/10.1038/s41467-023-42297-0

Macierzanka, A., Torcello-Gómez, A., Jungnickel, C., et al. (2019). Bile salts in digestion and transport of lipids. *Advances in Colloid and Interface Science, 274*, Article 102045. https://doi.org/10.1016/j.cis.2019.102045

Malektaj, H., Drozdov, A. D., & Christiansen, J.d. (2023). Swelling of homogeneous alginate gels with multi-stimuli sensitivity. *International Journal of Molecular Sciences, 24*, 5064. https://doi.org/10.3390/ijms24065064

Maljaars, P. W. J., Romeyn, E. A., Haddeman, E., Peters, H. P. F., & Masclee, A. A. M. (2009). Effect of fat saturation on satiety, hormone release, and food intake. *American Journal of Clinical Nutrition, 89*, 1019–1024. https://doi.org/10.3945/ajcn.2008.27335

McClements, D. J., & Li, Y. (2010). Review of in vitro digestion models for rapid screening of emulsion-based systems. *Food Funct, 1*(1), 32–59. https://www.ncbi.nlm.nih.gov/pubmed/21776455.

McClements, D. J., & Xiao, H. (2012). Potential biological fate of ingested nanoemulsions: Influence of particle characteristics. *Food & Function, 3*, 202–220. https://doi.org/10.1039/C1FO10193E

Mulet-Cabero, A.-I., & Wilde, P. J. (2023). Role of calcium on lipid digestion and serum lipids: A review. *Critical Reviews in Food Science and Nutrition, 63*, 813–826. https://doi.org/10.1080/10408398.2021.1954873

Ni, Y., Gu, Q., Li, J., et al. (2021). Modulating in vitro gastrointestinal digestion of nanocellulose-stabilized pickering emulsions by alternating cellulose lengths. *Food Hydrocolloids, 118*, Article 106738. https://doi.org/10.1016/j.foodhyd.2021.106738

Okuro, P. K., Viau, M., Marze, S., et al. (2023). In vitro digestion of high-lipid emulsions: Towards a critical interpretation of lipolysis. *Food & Function, 14*, 10868–10881. https://doi.org/10.1039/D3FO03816E

Patel, A. R., Babaahmadi, M., Lesaffer, A., et al. (2015). Rheological profiling of organogels prepared at critical gelling concentrations of natural waxes in a triacylglycerol solvent. *Journal of Agricultural and Food Chemistry, 63*, 4862–4869. https://doi.org/10.1021/acs.jafc.5b01548

Patton, J. S., & Carey, M. C. (1979). Watching fat digestion. *Science, 204*, 145–148. https://www.jstor.org/stable/1747578.

Rungraung, N., Jain, S., Mitbumrung, W., et al. (2022). Controlling the in vitro gastrointestinal digestion of emulsified lipids by encapsulation within nanocellulose-fortified alginate beads. *Food Structure, 32*. https://doi.org/10.1016/j.foostr.2022.100266

Sarkar, A., Ye, A., & Singh, H. (2016). On the role of bile salts in the digestion of emulsified lipids. *Food Hydrocolloids, 60*, 77–84. https://doi.org/10.1016/j.foodhyd.2016.03.018

Sarkar, A., Zhang, S., Holmes, M., et al. (2019). Colloidal aspects of digestion of pickering emulsions: Experiments and theoretical models of lipid digestion kinetics. *Advances in Colloid and Interface Science, 263*, 195–211. https://doi.org/10.1016/j.cis.2018.10.002

Scheuble, N., Schaffner, J., Schumacher, M., et al. (2018). Tailoring emulsions for controlled lipid release: Establishing in vitro−in vivo correlation for digestion of lipids. *Applied Materials & Interfaces, 10*, 17571–17581. https://doi.org/10.1021/acsami.8b02637

Schroën, K., Wu, L., & Corstens, M. (2022). Food-grade microgel capsules tailored for anti-obesity strategies through microfluidic preparation. *Current Opinion in Food Science, 45*, Article 100816. https://doi.org/10.1016/j.cofs.2022.100815

Smit, H., Keenan, E., Kovacs, E., et al. (2011). No efficacy of processed fabuless (olibra) in suppressing appetite or food intake. *European Journal of Clinical Nutrition, 65*, 81–86. https://doi.org/10.1038/ejcn.2010.187

Tan, Y., Zhang, Z., Liu, J., et al. (2020a). Factors impacting lipid digestion and nutraceutical bioaccessibility assessed by standardized gastrointestinal model (infogest): Oil droplet size. *Food & Function, 11*, 9936–9946. https://doi.org/10.1039/D0FO01505A

Tan, Y., Zhang, Z., Mundo, J. M., et al. (2020b). Factors impacting lipid digestion and nutraceutical bioaccessibility assessed by standardized gastrointestinal model (infogest): Emulsifier type. *Food Research International, 137*, Article 109739. https://doi.org/10.1016/j.foodres.2020.109739

Torcello-Gómez, A., Boudard, C., & Mackie, A. R. (2018). Calcium alters the interfacial organization of hydrolyzed lipidsduring intestinal digestion. *Langmuir, 34*, 7536–7544. https://doi.org/10.1021/acs.langmuir.8b00841

van Leusden, P., den Hartog, G. J. M., Bast, A., et al. (2018). Lipase diffusion in oil-filled, alginate micro- and macrobeads. *Food Hydrocolloids, 85*, 242–247. https://doi.org/10.1016/j.foodhyd.2018.07.028

Verkempinck, S. H. E., Salvia-Trujillo, L., Moens, L. G., et al. (2018). Kinetic approach to study the relation between in vitro lipid digestion and carotenoid bioaccessibility in emulsions with different oil unsaturation degree. *Journal of Functional Foods, 41*, 135–147. https://doi.org/10.1016/j.jff.2017.12.030

Verkempinck, S. H. E., Salvia-Trujillo, L., Moens, L. G., et al. (2018). Emulsion stability during gastrointestinal conditions effects lipid digestion kinetics. *Food Chemistry, 246*, 179–191. https://doi.org/10.1016/j.foodchem.2017.11.001

Visser, C. W., Kamperman, T., Karbaat, L. P., et al. (2018). In-air microfluidics enables rapid fabrication of emulsions, suspensions, and 3d modular (bio)materials. *Science Advances, 4*. https://doi.org/10.1126/sciadv.aao1175

Wang, P., Wang, H., Hou, Y., et al. (2023). Formation and in vitro simulated digestion study of gelatinized Korean pine seed oil encapsulated with calcified wax. *Molecules, 28*, 7334. https://doi.org/10.3390/molecules28217334

Wilbrink, J., Masclee, G., Klaassen, T., et al. (2021). Review on the regional effects of gastrointestinal luminal stimulation on appetite and energy intake: (pre)clinical observations. *Nutrients, 13*, 1601. https://doi.org/10.3390/nu13051601

Wooster, T. J., Acquistapace, S., Mettraux, C., et al. (2019). Hierarchically structured phase separated biopolymer hydrogels create tailorable delayed burst release during gastrointestinal digestion. *Journal of Colloid and Interface Science, 553*, 308–319. https://www.ncbi.nlm.nih.gov/pubmed/31212230.

Wu, L., Schroën, K., & Corstens, M. (2024). Structural stability and release properties of emulsion-alginate beads under gastrointestinal conditions. *Food Hydrocolloids, 150*, Article 109702. https://doi.org/10.1016/j.foodhyd.2023.109702

Wu, Q., Zhang, T., Xu, Y., et al. (2017). Preparation of alginate coreeshell beads with different m/g ratios to improve the stability of fish oil. *LWT - Food Science and Technology, 80*, 304–310. https://doi.org/10.1016/j.lwt.2017.01.056

Zangenberg, N. H., Mullertz, A., Kristensen, H. G., et al. (2001). A dynamic in vitro lipolysis model i. Controlling the rate of lipolysis by continuous addition of calcium. *European Journal of Pharmaceutical Sciences, 14*, 115–122. https://doi.org/10.1016/S0928-0987(01)00169-5

Zhang, X., Qu, Q., Zhou, A., et al. (2022). Core-shell microparticles: From rational engineering to diverse applications. *Advances in Colloid and Interface Science, 299*, Article 102568. https://www.ncbi.nlm.nih.gov/pubmed/34896747.

Zhang, Z., Zhang, R., Zou, L., et al. (2016). Encapsulation of curcumin in polysaccharide-based hydrogel beads: Impact of bead type on lipid digestion and curcumin bioaccessibility. *Food Hydrocolloids, 58*, 160–170. https://doi.org/10.1016/j.foodhyd.2016.02.036